Journal of GeoEngineering, Vol. 12, No. 3, pp. 119-127, September 2017
http://dx.doi.org/10.6310/jog.2017.12(3).3

ANALYTICAL SOLUTION TO THE PROBLEM OF PASSIVE SHAFT RESISTANCE DUE TO LOWERING OF GROUNDWATER TABLE

Ala N. Aljorany [1]

ABSTRACT

Lowering of groundwater table (GWT) is ordinarily accompanied by soil compression. The increase in the effective overburden stress is the main reason behind this compression. The submerged unit weight of soil before the lowering of GWT changes to the total unit weight along the dewatered depth. Analysis of the passive shaft resistance (PSR) that is often induced along the shaft of an existing pile in such a consolidating soil is the main subject of this study. After imposing the calculated distribution of final soil compression along the pile length, the governing differential equation of the pile displacement problem is analytically solved. By means of the obtained solution, the pile displacement, axial load and the induced PSR are expressed as continuous functions along the pile length. The proposed solution is first applied to analyze a reported case in which field measurements of the soil settlement, the pile top displacement and the dissipation of excess pore water pressure were continuously monitored for a time period of 260 days after pile driving. The finite element method is utilized as well to solve the whole behavior of the pile-soil system. The obtained results agree well with the measured values of pile displacement and soil settlement and with those obtained by the finite element method. The present solution is then utilized to perform a parametric analysis to investigate the most important parameters that affect the induced PSR. It is found that the depth of dewatered zone has a significant effect on the magnitude of the induced PSR. It is realized also that the depth of the neutral plane, where both the pile and the surrounding soil are displaced equally, gets close to the pile tip as the stiffness of the bearing layer below the pile base becomes great.

Key words: Soil compression, lowering of groundwater table, pile, passive shaft resistance, analytical solution.

1. INTRODUCTION

Piled foundations are ordinarily used wherever a problem of high compressibility or insufficient bearing capacity is encountered in the upper, relatively thick soil strata. Piles transfer the loads of superstructures to the soils through two components, namely, the base resistance and the skin friction. In more recent terminology, the older expression of "skin friction" is replaced by "shaft resistance" (Fellenius 1984). For axially loaded piles, the amounts of the mobilized shaft and base resistances depend mainly on the relative displacement between the pile and the soil. Depending on the soil type, a relative displacement of (0.2% ~ 2%) of the pile diameter could be quite enough to mobilize the full shaft resistance (Fleming *et al*. 2009).

In many practical situations, the soil in the pile vicinity is displaced vertically and/or horizontally due to different natural or artificial causes. For instances, seasonal variation of groundwater (inundation or drying) may cause soil swelling or shrinkage. Manmade activities such as a nearby construction, excavation or groundwater withdrawal are usually accompanied by soil movements. In such situations, the piles are usually subjected to passive loading conditions that may not been accounted for in the early stages of the piled foundation design. As a result of the surrounding soil compression, the pile often undergoes a state of the so called "negative skin friction" (NSF). In the author's mind, it is more convenient to identify this phenomenon as passive shaft resistance (PSR) rather than NSF to differentiate it from the (active) shaft resistance which is normally produced when the pile is displaced due to the application of an external load at its head. The PSR could be positive or negative depending on the direction of soil movement (swelling or compression). Even for a specific direction of soil movement, the direction of the PSR may change from negative to positive or vice versa along the pile depth. This change in the PSR direction occurs at the neutral plane (NP) where the pile and the surrounding soil are equally displaced so that there is no relative displacement between pile and soil. However, Johannessen and Bjerrum (1965), Fellenius and Broms (1969) and Bozozuk (1972) reported measurements of NSF dragloads that are greater than the allowable loads that are ordinarily applied to the piles.

Many of early studies on the NSF problem are dated back to the fifties of the past century. Zeevaert (1959) suggested a theoretical approach to evaluate the load capacity of end bearing piles subjected to NSF taking into account the reduction of the confining pressure at the bearing stratum which was attributed to the hang-up tendency of the settling soil. By employing Mindlin's equation for the vertical displacement of a point load within a semi- infinite mass, Poulos and Mattes (1969) proposed an analytical method to predict the effects of NSF on a single pile. Feda (1976) proposed expressions to determine the depth of the neutral

Manuscript received January 3, 2017; revised May 31, 2017; accepted June 1, 2017.
[1] Professor (corresponding author), Department of Civil Engineering, University of Baghdad, Al-Jaderriya, Baghdad, Iraq (e-mail: alaljorany@gmail.com).

plane and the average negative and positive skin frictions. Based on a theoretical approach, Janbu (1976) presented a method for determining the bearing capacity of friction piles embedded in a settling soil including a procedure for estimating the accompanying NSF. Bozozuk (1981) presented a semi-empirical method to determine the down-dragload for piles subjected to highway embankment surcharge. The NSF was related to the horizontal effective stress acting on the pile. By extending the work of Randolph and Worth (1978), Fleming *et al*. (2009) derived an analytical method to determine the distribution of NSF on the pile shaft. The method is based on the load transfer approach which involves the hypothesis of considering the pile is surrounded by concentric soil cylinders. The magnitude of the induced shear stress on the surface of each cylinder varies inversely with its radius. This load transfer approach will be adopted in this study to obtain an analytical solution to the differential equation that governs this problem. Kong *et al.* (2013) presented a simple semi-empirical mathematical model to analyze and calculate the dragload of pile group embedded in a consolidating soil. The model is based on Davis consolidation theory (Davis and Raymond 1965) and adopts a hyperbolic load transfer model for pile-soil interface. Practical case studies were analyzed by using this model and the results indicate that the predicted values of dragload were found to be in good agreement with the measured values.

In addition, there are many studies in the literature that deal with the NSF problem by using numerical approaches, particularly, the finite element method. Lee *et al*. (2002) performed a two and three dimensional finite element analyses for an individual pile and a pile group, respectively. The soil slip at the pile-soil interface was found to be the most important factor that governs the pile behavior in a consolidating soil. By using a two dimensional axisymmetric finite element model, Liu *et al.* (2012) found that the distribution and magnitude of NSF is influenced mainly by the pile/soil interface, soil compressibility, and the surcharge intensity. Rodríguez-Rebolledo *et al*. (2015) have simulated friction piles in typical Mexico City soft clays as an axi-symmetric problem considering external loads and soil consolidation due to variations in piezometric conditions. The analysis results show that due to soil consolidation, a neutral level separating positive skin friction from negative skin friction develops on the pile shaft. The position of this level depends more on pile spacing than on the magnitude of the pore pressure drawdown. For close pile spacing, the neutral level is near the pile tip and the piles can protrude from the consolidating surrounding soil as a result of regional subsidence. Three dimensional nonlinear analyses using ABAQUS 6.12 have been performed by Fathi and Naema (2015) to analyze and quantify the dragload and down drag imposed on single pile installed in a consolidating soil. Analysis results revealed that sacrificing piles, which are unloaded piles, ‘‘hang up’’ the soil between the piles in the group and thus, the vertical effective stress around the shielded pile is reduced. An experimental work on pile NSF is carried out by Shen *et al*. (2013). In that study, a centrifuge model is used to investigate the behavior of pile subjected to NSF induced by pile installation, groundwater drawdown and surcharge loading. A finite element model is first validated against the centrifuge test results and then extended to investigate the effects of pile slenderness ratio, surcharge intensity and pile- soil stiffness ratio on the degree of mobilization of NSF induced on the pile.

In the present research, the profile of soil compression resulting from lowering of groundwater table is dealt with as the source of passive shaft resistance (PSR) along a pile. An analytical solution is presented to evaluate the distribution of PSR, axial load and displacement along the pile. In addition, the depth of neutral plane is analytically determined and the main factors that affect this depth are parametrically investigated.

2. PROBLEM STATEMENT AND MATHEMATICAL MODELING

Considering the soil profile shown in Fig. 1, the groundwater table is initially at the natural ground surface level. The vertical effective stress (σ'_v) at any point at depth (z) can simply be calculated as $\sigma_v' = \gamma_b \cdot Z$, where γ_b is the buoyant (submerged) unit weight of soil. As the water table is lowered to the depth (H), the soil unit weight above that depth will be (γ_t) which is much greater than γ_b. Depending on the soil type and the amount of the residual water content, the difference ($\gamma_t - \gamma_b$) which is denoted as $\tilde{\gamma}$ is normally ranging between 5 and 10 kN/m^3. This implies that the vertical effective stress at any point below the depth H will increase by the amount $\tilde{\gamma}\,H$, and the resulting settlement S along that depth can be calculated by the integral $\int_z^L m_v \tilde{\gamma}\, Hdz$, where m_v is the coefficient of soil volume change which is the reciprocal of the constraint modulus, and L represents the total depth of the consolidating soil which will be used later as the pile embedded depth.

In addition, the vertical effective stress above that depth will increase also by an amount which varies along that depth and can be calculated by the integral $\int_z^H m_v \tilde{\gamma}\, zdz$. Eventually, the final consolidation settlement (S) expressed as a function of the depth (z) is obtained as follows:

$$S(z) = S_H + S_O\left[1-(z/H)^2\right] \quad \text{for} \quad 0 \le z \le H \tag{1}$$

and

$$S(z) = S_H\left(\frac{L-z}{L-H}\right) \quad \text{for} \quad H \le z \le L \tag{2}$$

where $S_H = m_v \tilde{\gamma} H(L-H)$ and $S_O = 0.5 m_v \tilde{\gamma} H^2$.

The variation of the final settlement of soil with depth is also shown in Fig. 1.

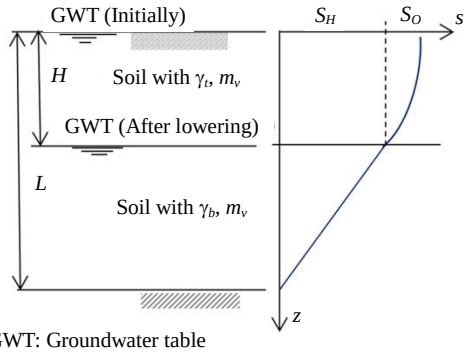

Fig. 1 Problem statement and parameter definitions

Supposing that an individual pile is existing in such a consolidating soil, it will tend to resist the soil compression since its stiffness is ordinarily higher than that of the surrounding soil. A state of PSR will then be generated along the pile shaft. Figure 2 shows the pile displacement in a consolidating soil and a pile element of length Δz. By considering the equilibrium of forces that act on the pile element, the following equation is obtained:

$$\frac{dP(z)}{dz} = \pi D \tau_s(z) \tag{3}$$

where D is the pile diameter, P and τ_s are the pile axial force and the unit shaft resistance expressed as functions of the depth z, respectively. By applying the Randolph and Wroth (1978) hypothesis, the soil vertical displacement w_s at any radial distance r from the pile axis can be expressed as:

$$w_s(r, z) = S(z) - \frac{D \cdot \tau_s(z)}{2G_s} \ln(r_m / r) \tag{4}$$

where G_s is the soil shear modulus and r_m is the radius of pile influence zone. Assuming that there is no slippage between pile and soil at the pile-soil interface, Eq. (4) can be used to calculate the pile displacement w by substituting r by $D/2$ to get:

$$w(z) = S(z) - \frac{D \cdot \tau_s(z)}{2G_s} \ln(2r_m / D) \tag{5}$$

or

$$\tau_s(z) = \frac{2G_s}{D\zeta}\left[S(z) - w(z)\right] \tag{6}$$

where $\zeta = \ln(2r_m/D)$. The value of ζ is ranging between 3 and 5 (Fleming *et al*. 2009) and by substituting Eq. (6) into Eq. (3) one can get:

$$\frac{dP(z)}{dz} = \frac{2\pi G_s}{\zeta}\left[S(z) - w(z)\right] \tag{7}$$

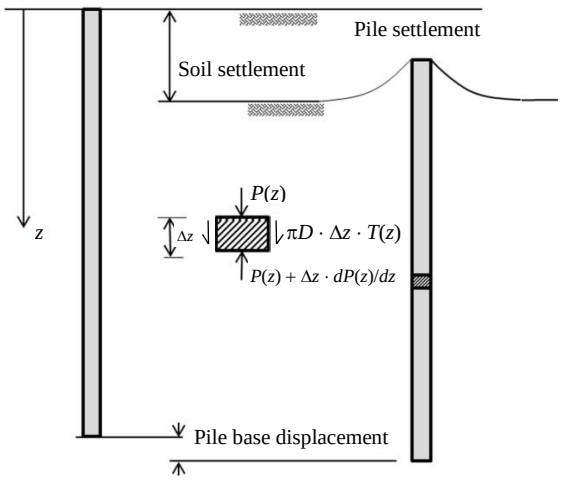

Fig. 2 Soil settlement and pile displacement in a consolidating soil

Since the axial force at any section along the pile $P(z)$ can be expressed as:

$$P(z) = -EA\frac{dw(z)}{dz} \tag{8}$$

where E is the pile modulus of elasticity and A is the pile cross sectional area, then:

$$EA\frac{d^2w(z)}{dz^2} = -\frac{2\pi G_s}{\zeta}\left[S(z) - w(z)\right] \tag{9}$$

or by re-arranging:

$$\frac{d^2w(z)}{dz^2} - \lambda^2 w(z) = -\lambda^2 S(z) \tag{10}$$

where $\lambda^2 = 2\pi G_s/\zeta EA$.

Considering the soil displacement given in Eqs. (1) and (2), the governing differential Eq. (10) will be:

$$\frac{d^2w(z)}{dz^2} - \lambda^2 w(z) = \lambda^2 S_H\left[\alpha(z/H)^2 - \alpha - 1\right] \text{ for } 0 \le z \le H \tag{11a}$$

$$\frac{d^2w(z)}{dz^2} - \lambda^2 w(z) = \lambda^2 S_H\left(\frac{z-L}{L-H}\right) \text{ for } H \le z \le L \tag{11b}$$

where α in Eq. (11a) equals (S_O/S_H). Equation (11) is a non-homogeneous differential equation which can be solved in two stages depending on the depth z. The solution is:

$$w(z) = c_1 e^{\lambda z} + c_2 e^{-\lambda z} + A1 + B1z + C1z^2 \quad 0 \le z \le H \tag{12a}$$

$$w(z) = c_3 e^{\lambda z} + c_4 e^{-\lambda z} + A2 + B2z \quad H \le z \le L \tag{12b}$$

The integration constants of the complementary solution are:

$$A1 = \alpha S_H\left[1 + \frac{1}{\alpha} - \frac{2}{(\lambda H)^2}\right], \quad B1 = 0, \quad C1 = -\frac{\alpha S_H}{H^2} \tag{13}$$

$$A2 = S_H\frac{L}{L-H} \quad \text{and} \quad B2 = -\frac{S_H}{L-H} \tag{14}$$

Whereas, the integration constants of the particular solution (c_1, c_2, c_3 and c_4) can be obtained by satisfying the following four boundary conditions:

- $EA\frac{dw(z)}{dz} = 0$ at z = 0, there is no axial force at the pile head.
- $w(z)$ from Eq. (12a) is the same as that obtained from Eq. (12b) at $z = H$ to satisfy the compatibility of pile displacement.
- The first derivative of $w(z)$ from Eq. (12a) is the same as that from Eq. (12b) at $z = H$, to satisfy the forces equilibrium at that pile section.
- $EA\frac{dw(z)}{dz} = -K_b w(z)$ at $z = L$, where K_b is the soil stiffness at the pile base.

Introducing the relative stiffness factor (μ) which is defined as $\mu = \lambda EA/K_b$ and solving for the integration constants gives:

$$c_4 = \frac{\frac{S_H}{\lambda H}(e^{\lambda H}+e^{-\lambda H})\left[\frac{H}{2(L-H)}+\alpha(1+\frac{1}{\lambda H})\right]-\frac{\mu S_H}{\lambda e^{\lambda L}(L-H)(\mu+1)}}{\frac{\mu-1}{\mu+1}e^{-2\lambda L}-1} \quad (15)$$

$$c_3 = c_4\frac{\mu-1}{\mu+1}e^{-2\lambda L}+\frac{\mu S_H}{\lambda e^{\lambda L}(L-H)(\mu+1)} \quad (16)$$

$$c_2 = c_1 = c_3-\frac{S_H}{\lambda H e^{\lambda H}}\left[\frac{H}{2(L-H)}+\alpha\left(1+\frac{1}{\lambda H}\right)\right] \quad (17)$$

After obtaining the complete analytical solution of the relevant problem, a Matlab M-file is constructed to perform the calculations and present the results as plots that demonstrate the variations of pile displacement, pile axial force and the distribution of PSR along the pile depth. In the following section, the present analytical solution is verified and its results are compared with field measurements and the finite element analysis of a reported problem in the literature.

3. VERIFICATION OF THE PRESENT SOLUTION

Many attempts have been made to find field measurements of pile and soil compression that are resulted from lowering of groundwater but unfortunately such measurements are very scarce in the available literature. One of the interesting studies that reported field measurements for soil consolidation and final settlement was presented by Blanchet *et al*. (1980). The study deals with the behavior of friction piles in soft sensitive clay. Among many other field measurements, the soil consolidation in the vicinity a group of four timber piles was monitored for a time period of 260 days before applying the pile dead load. The soil profile consists of a thick clayey silt to silty clay soil with undrained shear strength increases linearly with depth from less than 10 kPa close to the ground surface to 150 kPa at 55 m depth. During the pile driving, the generated excess pore water pressure was monitored at a radial distance of 0.56 m from the pile axis. Each of the four piles has a length of 15.85 m and average diameter of 0.293 m. The measured values of excess pore water pressure $\Delta u/\sigma'_p$ at depths of 9.5 m and 13.6 m was ranging from 0.8 to 1.2. The variation of effective pre-consolidation pressure (σ'_p) with depth is linear and almost equal to that of the effective overburden pressure (σ'_v) since the soil is normally to lightly overconsolidated. After 260 days, the soil settlement was recorded at three points along the pile axis. The measured values are: 40 mm, 30 mm and 10 mm at depths of 3.3 m, 9.2 m and 14.1 m, respectively. The pile head settlement at the end of that time period was 22 mm. Blanchet *et al*. (1980) reported that such distribution of pile and soil settlement clearly indicated the development of a negative skin friction condition in the upper 12 m (about 75%) of the pile length, and a positive skin friction condition in the lower 25% of the piles length. As a result of this dragload on the piles, the pile tip is displaced downward at least 15 mm (Blanchet *et al*. 1980).

It is obvious that the field measurements in this case study are limited to soil settlement at three different depths, pile head settlement and the pore water pressure in the vicinity of pile. The finite element method is therefore used in this study to to analyze the problem and figure out the whole behavior of pile- soil system and the generated PSR. The finite element package (ABAQUS 6.13) is used in the analysis. The problem is treated as an axi-symmetric one with three analysis steps. In the first, the geometric boundary conditions and the initial level of groundwater table are defined. The second step which is called (Geostatic) is the very important to calculate the initial geostatic stresses and the pore water pressure. In the third step, the water table is lowered down to the pile tip and the resulting displacements and stresses of the soil and pile are obtained at different locations. In order to be consistent with the assumption of the analytical solution, full contact between pile and soil has been used to model the pile-soil interface.

Figure 3 displays the finite element mesh of the problem and the contours of the vertical displacement that occurs after lowering the GWT from ground surface down to the pile tip. It can be noticed that the pattern of soil vertical displacement in the vicinity of the pile is considerably influenced by the presence of pile which is relatively stiffer than the surrounding soil.

Although this selected case study is not very related to soil compression due to lowering of GWT, the proposed solution can be applied to analyze the induced PSR considering the following hypothesis. It is known that the initial excess pore water pressure will dissipate with time and at the end of the consolidation process the final vertical effective stress will eventually increase by the same amount of the initial excess pore water pressure. Considering the average value for the initial excess pore water pressure of $\Delta u/\sigma'_o \approx 1$, where σ'_o denotes the initial (in situ) effective stress as mentioned by Blanchet *et al*. (1980), this implies that the final effective stress at each depth will increase by an amount equals to its initial value. In effect, such increase in the effective stress is equivalent to that produced by doubling the effective unit weight of the consolidating soil. In order to apply the current solution, the value of $\tilde{\gamma}$ in Eq. (12a) will therefore be equals to the buoyant unit weight ($\gamma_b \approx 10$ kN/m^3) for the whole soil layer along the pile depth. Regarding other soil and pile properties, the soil shear modulus G_s is considered as 150 C_u and its Poisson's ratio (v) is 0.45. The value of m_v can then be calculated as $(1-2v)/2G_s(1-v)$. The pile modulus of elasticity E is given by Blanchet *et al.* (1980) as 6.9×10^6 kPa.

The results of the present analytical solution, the finite element analysis and the field measurements regarding soil final consolidation are displayed in Fig. 4. The pile axial force in this figure is normalized by the pile sectional property (EA), while the shear stress that is generated due to PSR, is normalized by the soil shear modulus (G_s).

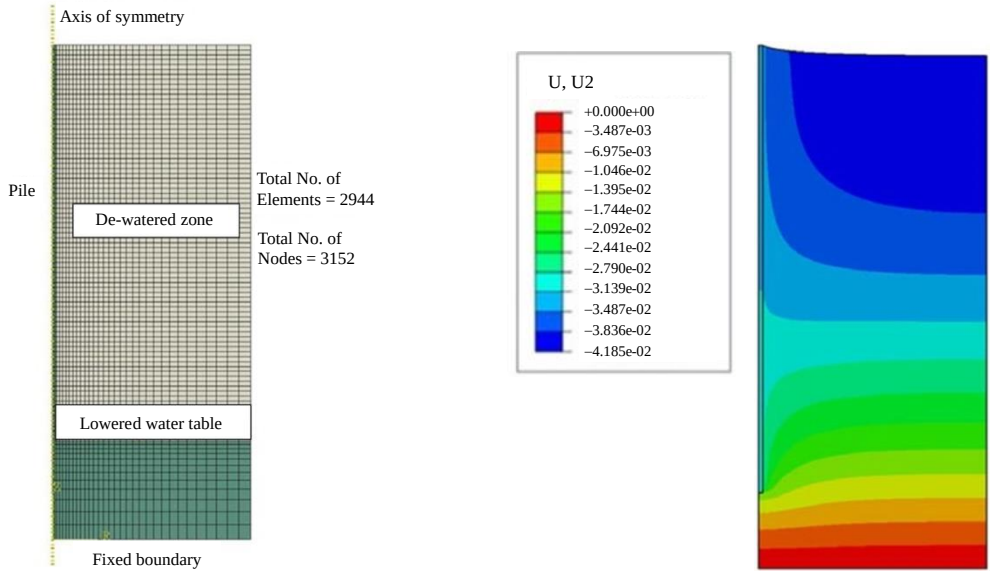

(a) Finite element mesh (b) Contour of vertical displacement

Fig. 3 The finite element mesh of the problem and the contour of vertical displacements

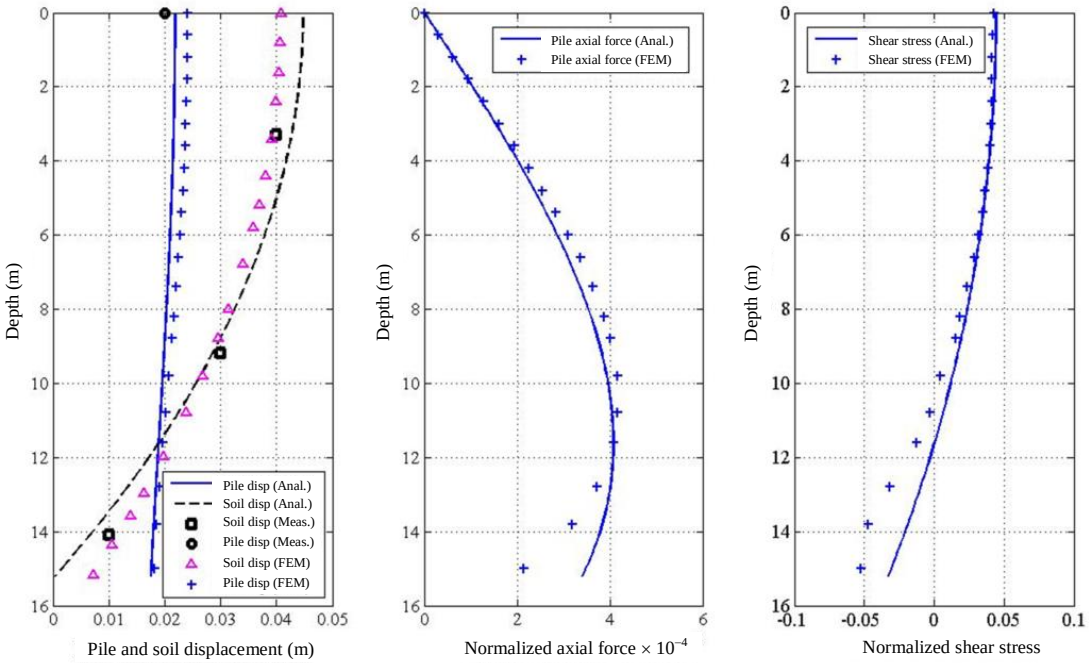

Fig. 4 Variation of measured and calculated soil settlement, pile displacement, axial load and PSR with depth

From Fig. 4(a), it can be noticed that the general trend of variation of the soil settlement with depth which is calculated by the present analytical solution, agree well the measured one and with that obtained by the finite element analysis. This finding is an essential step since the proposed analytical solution is mainly dependent on the profile of soil movement. The calculated pile head settlement which is about 22 mm is almost equal to the measured value but the pile base settlement which is about 17 mm is slightly greater than that estimated by Blanchet *et al*. (1980). It is worth mentioning that the obtained depth of neutral plane is about 11.6 m (73% of the pile length). The estimated neutral plane depth as given by Blanchet *et al*. (1980) is 12 m, or about 75% of the pile length. Since there was no instrumentation to measure the induced axial load or the generated PSR along the pile, the finite element results shown in Figs. 4(b) and 4(c) indicate good agreement with the results of the present analytical solution. The slight deviation near pile tip could be attributed to compression of soil below the pile tip in the finite element analysis. In Fig. 4(c), the point at which the PSR changed from negative to positive is clearly defined and coincides with that at which the soil settlement and pile displacement becomes equal. It can therefore be concluded that the results of the present analytical solution fit well with the reported field measurements and the finite element results in terms of soil settlement and pile displacement.

4. PARAMETRIC ANALYSIS OF THE PSR PRODUCED BY WATER TABLE LOWERING

It is thought that little or no serious attention is paid in the literature to soil compression resulting from water table lowering. This compression may cause structural damages to the nearby structures and produce PSR along the piles that are embedded in such soils. It is therefore worthy to investigate the most important parameters that affect PSR magnitude and distribution along the pile. The results of a parametric analysis that has been performed by utilizing the present analytical solution, are presented and discussed in the following sections.

4.1 Effects of the Depth of Lowering of Groundwater Table

Different values for the depth of GWT lowering (H) have been examined in the present analysis to evaluate the effects of this parameter on the soil settlement, pile displacement, axial force and the induced PSR. In Fig. 5 and the following figures, the GWT lowering depth H and the depth of neutral plane are presented as a ratio of the pile length L. The soil settlement and pile displacement are expressed as ratios of the pile diameter D. The pile axial force and the induced passive shear stress are normalized by the pile axial rigidity (EA) and the soil shear modulus (G_s), respectively.

From Fig. 5(a), it can be noticed that both soil settlement and pile displacement increase with a decreasing rate as the depth of GWT lowering (H) increases. The relative displacement between pile and soil gets greater as well. The depth ratio of neutral plane as shown in Fig. 5(b) changes from 0.55 to 0.65 as the value of H changes from 0.2L to L. At a lowering depth of slightly greater than 0.62L, the neutral plane reaches the same depth (H). Figure 5(c) indicates that the maximum axial force which always occurs at the same level of the neutral plane increases almost linearly with H up to about 0.6L, then its increasing rate becomes slower to be insignificant for lowering depths greater than 0.8L. Regarding the induced passive shear stress, its maximum value which occurs at the ground level becomes greater as the lowering depth increases. The same trend of maximum axial force variation is noticed for the maximum passive shear stress. It can therefore be deduced that for lowering depths greater than 0.8L the quantitative changes in the induced PSR and its effects become insignificant.

4.2 Effects of the Relative Stiffness Between the Pile and the Surrounding Soil

Referring to the definition of the parameter λ given in Eq. (10), the parameter λL can be used as a non-dimensional parameter that relates the pile stiffness to that of the surrounding soil. Fleming *et al*. (2009) used a similar parameter to indicate whether the pile behaves as a rigid (short) or compressible (long) pile depending on the value of slenderness ratio (L/D). It is simply if $L/D \le 0.25\ (E/G_s)^{0.5}$ the pile then behaves as a rigid pile otherwise it behaves as a compressible pile. For $L/D \ge 1.5\ (E/G_s)^{0.5}$ the pile will behave as a very compressible. Basing on the same criteria, the parameter λL is obtained in this study so that the pile exhibits a compressible behavior for the range of ($0.33 \le \lambda L \le 2$). Below the lower limit, the pile behaves as a rigid pile and above the upper limit it becomes very compressible. In order to evaluate the effect of this parameter on the induced PSR, the soil parameters, pile length and diameter are kept constant. The depth of GWT lowering is considered as half the pile length (L/2). The change in λ is manipulated by changing the value of pile modulus of elasticity E.

Figure 6 illustrates the effects of changing λL on the induced PSR and its consequences. The almost rigid behavior of the pile can be noticed in Fig. 6(a) where the difference between pile top and base displacements becomes insignificant for the values of λL smaller than 0.33. Consequently, the maximum axial force shown in Fig. 6(c) is relatively small at this range of λL because of the relatively small values of the pile axial strain. As the value of λL becomes greater, the pile head displacement increases while pile base displacement decreases to indicate a pronounced compression in the pile body.

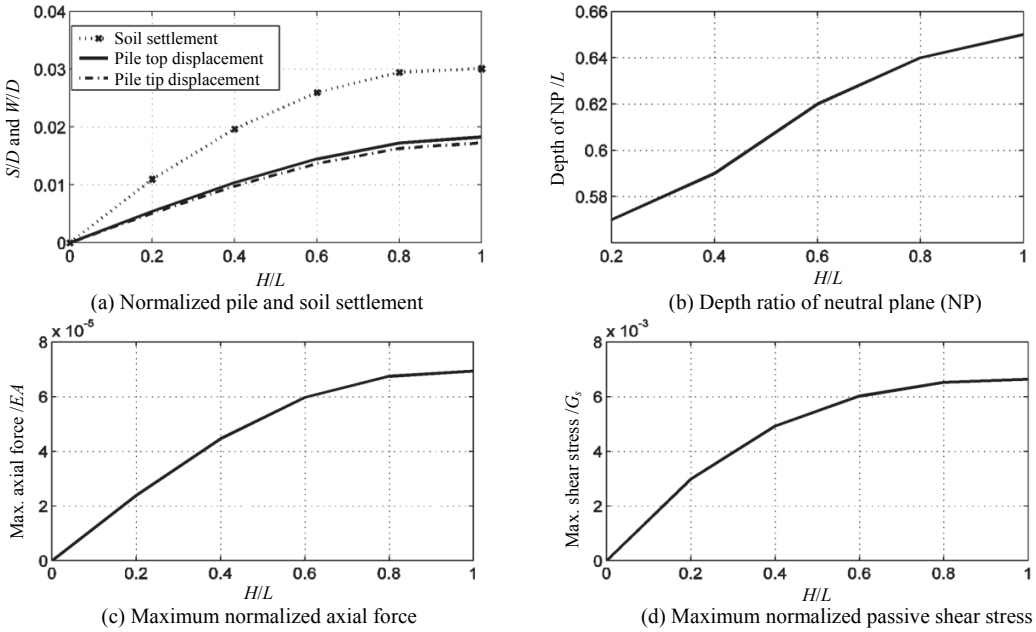

(a) Normalized pile and soil settlement

(b) Depth ratio of neutral plane (NP)

(c) Maximum normalized axial force

(d) Maximum normalized passive shear stress

Fig. 5 Effects of GWT lowering depth (H) on the soil and pile displacements, the depth ratio of neutral plane, the maximum axial force and the maximum passive shear stress

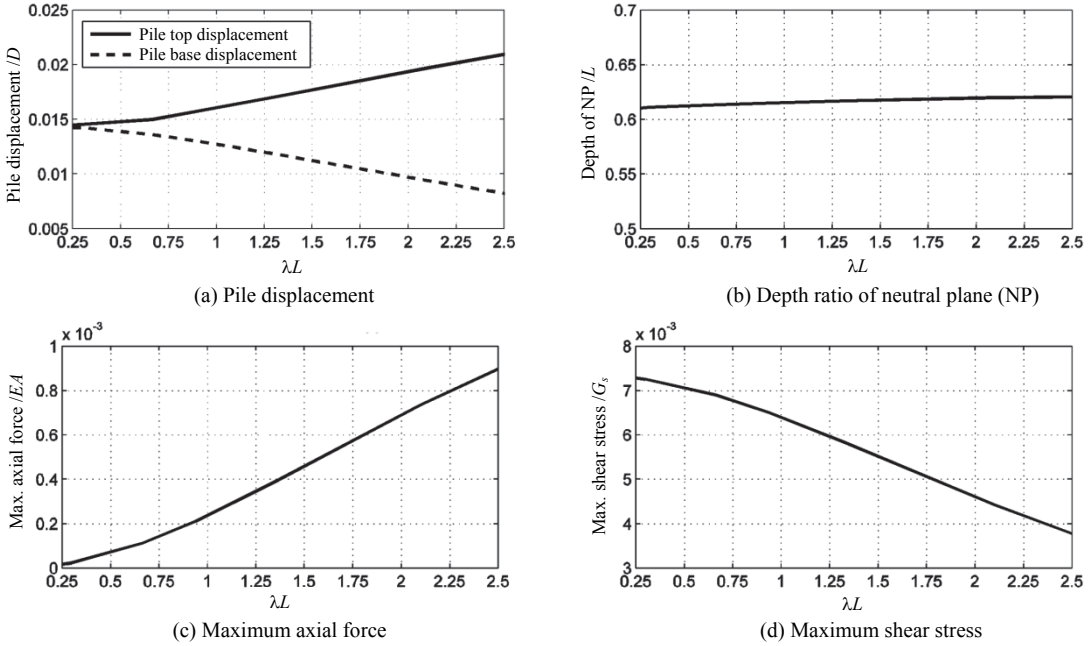

(a) Pile displacement (b) Depth ratio of neutral plane (NP)

(c) Maximum axial force (d) Maximum shear stress

Fig. 6 Effects of the relative stiffness parameter (λL) on the pile displacement, the depth ratio of neutral plane, the maximum axial force and the maximum passive shear stress

This finding is obviously reflected on the value of maximum axial force shown in Fig. 6(c) that increases significantly as λL gets greater. Regarding the effect of λL on the depth ratio of the neutral plane, Fig. 6(b) indicates insignificant changes in this ratio whether the pile behaves as a short (rigid) or long (compressible) pile. Figure 6(d) displays the variation of the maximum passive shear stress with λL. It can be noticed that the value of this stress decreases significantly as λL increases. This change can be explained by referring to Eq. (6), in which the value of passive shear stress depends principally on the relative displacement between the pile and the surrounding soil. As the pile gets more compressible, its displacement becomes greater as indicated in Fig. 6(a) and the relative displacement between the pile and the soil gets smaller since the soil settlement distribution along the pile is kept unchanged.

To shed more light on the distribution of displacement and stresses that are generated along the pile length due to the induced PSR, Fig. 7 displays this distribution for three different values of the relative stiffness parameter λL. For almost rigid pile where λL equals 0.25, the solid line depicts this behavior in terms of the pile top and pile base displacements. The other dashed and dotted lines in Fig. 7 illustrate the behavior of compressible pile (λL = 1) and very compressible pile (λL = 2.5), respectively. The distributions of axial force and passive shear stress confirm the findings that explained in Fig. 6.

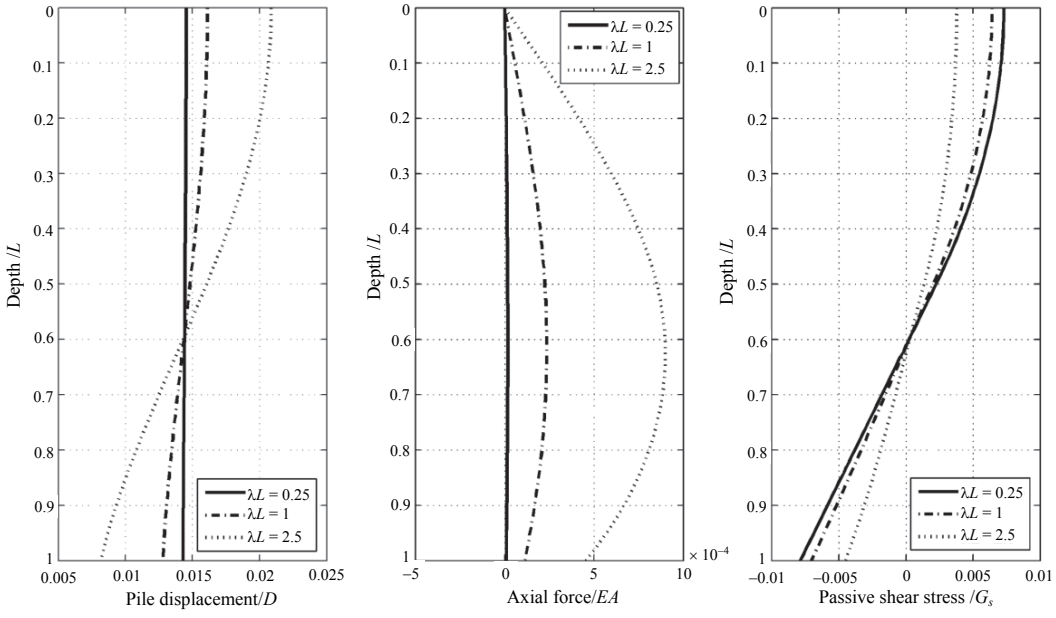

(a) Pile normalized displacement (b) Normalized axial force (c) Normalized passive shear stress

Fig. 7 Distributions of pile displacement, axial force and passive shear stress along the pile depth for three different values of the relative stiffness parameter λL

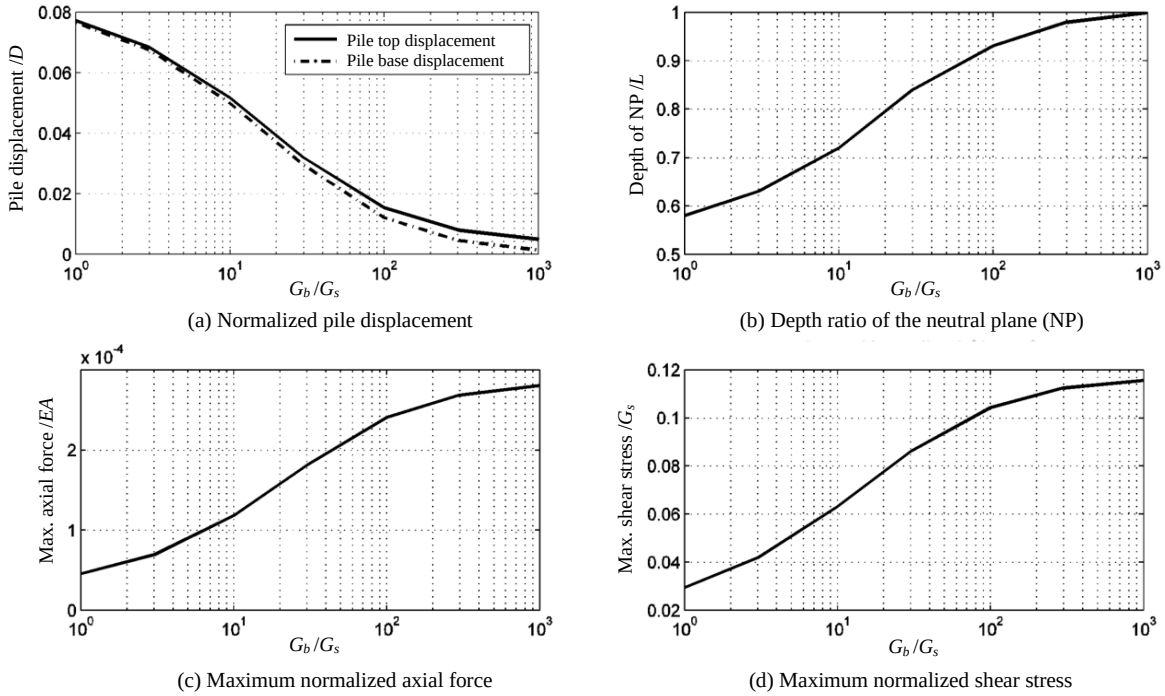

(a) Normalized pile displacement

(b) Depth ratio of the neutral plane (NP)

(c) Maximum normalized axial force

(d) Maximum normalized shear stress

Fig. 8 Effects of the bearing layer stiffness ratio G_b/G_s on the pile displacement, the depth ratio of neutral plane, the maximum axial force and the maximum passive shear stress

4.3 Effects of the Bearing Layer Stiffness

Many studies indicate that the bearing layer below the pile tip has significant effects on the induced PSR in a consolidating soil. In the present analysis, all of the soil and pile properties above the pile tip are kept unchanged. The relative stiffness of the bearing layer is expressed as the ratio of bearing layer shear modulus to that of the surrounding soil (G_b/G_s). A wide range of this ratio (from 1 to 1000) has been examined and the analysis results are displayed in Fig. 8 where this range is expressed in a logarithmic scale. Considerable decrease can be noticed in values of pile top and base displacement as the bearing layer stiffness increases but the difference between these two displacements becomes greater as shown in Fig. 8(a). From Fig. 8(b), the depth of neutral plane is highly affected by the stiffness of the bearing layer and changes from about 0.6L for $G_b/G_s = 1$ to the full pile length L for $G_b/G_s = 1000$. The same effects can be realized regarding the maximum axial force and the induced passive shear stress where they increase considerably with increasing the bearing layer stiffness as shown in Figs. 8(c) and 8(d). Three recognized patterns of variation are noticed in these figures. All the investigated parameters (pile displacement, depth of the neutral plane, axial force and passive shear stress) exhibit changes with an increasing rate for the range of ($1 \le G_b/G_s \le 10$). Almost a proportional variation is noticed in the range ($10 \le G_b/G_s \le 100$) and a decreasing rate of changes for ($100 \le G_b/G_s \le 1000$). Regarding the depth of the neutral plane, as this depth gets closer to the pile base, the case where the stiffness of the bearing layer becomes greater, the induced PSR becomes principally of a negative direction and higher portion of the dragload is transferred to the pile base.

5. CONCLUSIONS

An analytical solution is presented in this study to solve the governing differential equation of the problem of passive shaft resistance that is induced by soil compression resulting from lowering of groundwater table. By this solution, the pile displacement, axial force and the passive shear stress are expressed as continuous functions along the pile depth. The solution is verified by comparing its results with the field measurements that are reported by Blanchet *et al*. (1980). The finite element method is used to analyze the selected case study mainly to fill the gaps in the field measurements and present additional results for verification of the present analytical solution. A parametric analysis is then performed to investigate the most important parameters that affect the induced passive shaft resistance. The main conclusions that are deduced from this analysis are:

1. The depth of lowering of groundwater table has significant effects on the soil settlement, pile displacement and the induced passive shaft resistance. They increase with increasing depth until reaching 80% of the pile length. Beyond that depth, the effects become less pronounced.
2. For relatively rigid piles, the induced passive shaft resistance is greater than that produced in case of compressible piles. This may attributed to the amount of relative displacement between pile and soil which is higher for rigid piles than that of compressible ones.
3. The relative stiffness between the pile and the surrounding soil has insignificant effect on the depth of the neutral plane.
4. The stiffness of the bearing layer below the pile tip has pronounced effects on the magnitude and distribution of the induced passive shaft resistance along the pile length. For relatively stiff bearing layer, the induced PSR and the maximum axial force in the pile are greater than that relevant to a bearing layer of a lesser stiffness. The depth of neutral plane is highly influenced by the stiffness of the bearing layer and gets closer to the pile tip as this stiffness becomes greater compared to that of the surrounding soil.

REFERENCES

Blanchet, R, Tavenas, F.A., and Garneau, R. (1980). "Behavior of friction piles in soft sensitive clays." *Canadian Geotechnical Journal*, **17**(2), 203–224.

Bozozuk, M. (1972). "Downdrag measurements on a 160-ft floating pipe pile in marine clay." *Canadian Geotechnical Journal*, **9**(4), 127–136.

Bozozuk, M. (1981). "Bearing capacity of a pile preloaded by downdrag." *Proceedings of 10th International Conference on Soil Mechanics and Foundation Engineering*, Stockholm, **2**, 631–636.

Dassault Systemes Simulia Corporation (2013). *ABAQUS 6.13*, Providence, RI, USA.

Davis, E.H. and Raymond, G.P. (1965). "A non-linear theory of consolidation." *Geotechnique*, **15**(2), 161–173.

Abdrabbo, F.M. and Ali, N.A. (2015). "Behaviour of single pile in consolidating soil." *Alexandria Engineering Journal*, **54**(3), 481–495.

Feda, J. (1976). "Skin friction of piles." *Proceedings of 6th European Conference on Soil Mechanics and Foundation Engineering*, Vienna, **1-2**, 423–428.

Fleming, W.G.K., Weltman, A.J., Randolph, M.F., and Elson, W.K. (2009). *Piling Engineering*, 3rd Ed., Taylor and Francis, London, UK.

Fellenius, B.H. and Broms, B.B. (1969). "Negative skin friction for long piles driven in clay." *Proceedings of 7th International Conference on Soil Mechanics and Foundation Engineering*, Mexico, **2**, 93–98.

Fellenius, B.H. (1984). "Negative skin friction and settlement of piles." *Proceedings of 2nd International Seminar on Pile Foundations*, Nanyang Technological Institute, Singapore.

Janbu, N. (1976). "Static bearing capacity of friction piles." *Proceedings of 6th European Conference on Soil Mechanics and Foundation Engineering*, Vienna, **1.2**, 479–488.

Johannessen, I.J. and Bjerrum, L. (1965). "Measurement of the compression of a steel pile to rock due to settlement of the surrounding clay." *Proceedings of 6th International Conference on Soil Mechanics and Foundation Engineering*, Montreal, **2**, 261–264.

Kong, G., Liu, H., Yang, Q., Liang, R.Y., and Zhou, H. (2013). "Mathematical model and analysis of negative skin friction of pile group in consolidating soil." *Hindawi Publishing Corporation, Mathematical Problems in Engineering*, Volume 2013, Article ID 956076, 11 pages.

Lee, C.J., Bolton, M.D., and Al-Tabbaa, A. (2002). "Numerical modeling of group effects on the distribution of dragloads in pile foundations." *Geotechnique*, **52**(5), 325–335.

Liu, J., Gao, H., and Liu, H. (2012). "Finite element analyses of negative skin friction on a single pile." *Acta Geotechnica*, **7**(3), 239–252.

Poulos, H.G. and Mattes, N.S. (1969). "The analysis of downdrag in end bearing piles." *Proceedings of 7th International Conference on Soil Mechanics and Foundation Engineering*, Mexico, **2**, 203–209.

Randolph, M.F. and Wroth, C.P. (1978). "Analysis of deformation of vertically loaded piles." *Journal of the Geotechnical Engineering Division*, ASCE, **104**(12), 1465–1488.

Rodríguez-Rebolledo, J., Auvinet-Guichard, G., and Martínez-Carvajal, H. (2015). "Settlement analysis of friction piles in consolidating soft soils." *DYNA, Publication of Universidad Nacional de Colombia*, **82**(192), 211–220.

Shen, R.F., Leung, C.F., and Chow, Y.K. (2013). "Physical and numerical modeling of drag load development on a modelend-bearing pile." *Geomechanics and Engineering, An International Journal*, **5**(3), 195–221.

Zeevaert, L. (1959). "Reduction of point bearing capacity of piles because of negative skin friction." *Proceedings of 1st Pan-American Conference on Soil Mechanics and Foundation Engineering*, Mexico, **3**, 1145–1152.